Proceedings of the Institute of Acoustics

THE ADAPTIVE BEAM TRACING ALGORTIHM

IA Drumm University of Salford, Department of Acoustics and Electronic Engineering
YW Lam University of Salford, Department of Acoustics and Electronic Engineering

1 INTRODUTION

This paper describes the design and implementation of a new 'Adaptive Beam Tracing Algorithm' for the prediction of the acoustics of architectural enclosures. Current methods model propagating sound fields as rays, beams or images. These may produce holes or overlaps in the predicted sound field or require an unworkable CPU overhead for high orders of reflection. Hence a new method has been developed whereby the shape of reflected beams is governed by the shape of reflecting surfaces so as to produce a geometrically perfect description of the sound propagation. The method also facilitates the calculation of diffuse sound propagation by managing the energy transfer from a specular model to a diffuse model. This 'Adaptive Beam Tracing' method compares well with other methods in terms of speed and accuracy although is relatively difficult to implement successfully for complicated enclosures.

2 PREVIOUS METHODS

2.1 Overview

There are a number of different methods to predict the acoustics of auditoria. Unlike simple formulae for reverberation time based on hall volume, surface area and absorption (Sabine, Eyring, etc), the more sophisticated computer models attempt to describe interatively the process of sound propagation hence taking into account architectural shape and layout. The most popular methods are as follows.

2.2 Ray Tracing

Ray tracing (Kulowski[1]) creates a dense spread of rays, which are subsequently reflected around a room and tested for intersection with a spherical detector. The energy attenuation of the intersecting rays and distances travelled are used to construct an echogram. Although relatively simple to implement the algorithm has inherent systematic errors (Lehnert[2]) where by spurious reflections can be created due to using a non point detector whilst other valid reflections missed as the rays diverge.

2.3 The Image Method

The image method as demonstrated by Borish[3] and (Lee and Lee[4]) overcomes these problems by instead calculating images of the sound sources in reflecting walls. Higher order images are in turn calculated and so on until an echogram is produced. Although initially much faster than ray tracing the image method slows exponentially with increasing orders of reflection as the number of possible though not necessarily valid images increases. Invalid images must be eliminated with validity and visibility tests. Some applications such as Volander[5] use a hybrid of the two methods to improve speed and accuracy, however it still requires a large number of rays initially and suffers from missing images later on.

2.4 Beam Tracing

There are also conical (Maercke & Martin [6]) and triangular (Lewers[7]) beam tracing methods available. Beams are reflected around a room and tested for illumination of the detector. These algorithms provide the speed of ray tracing with the accuracy advantages of being able to use a point detector. However since cones and triangles represent approximations of the propagating sound field, overlaps and missing reflections can happen and so have to be compensated for statistically.

2 THE NEW METHOD

2.1 Overview

The adaptive beam tracing algorithm was developed to faithfully describe the specular propagating sound field without holes or overlaps. The shape of reflecting beams is based on the exact sections of illumination of previous beams on reflecting plane surfaces (Fig.1.), not triangular or conical approximations. Hence, the algorithm finds valid sound images as faithfully as the image method but without generating an exponential number possibilities to be eliminated with visibility tests. The adaptive beam tracing algorithm also facilitates a convenient way to calculate energy upon reflection by providing exact areas of illumination by beams on walls with respect to time. Diffuse energy imparted on walls can then be re-radiated and exchanged between walls so creating a diffuse echogram. Specular and diffuse components can then be combined so eliminating the need for empirical and statistical adjustments.

2.2 Representing 3D World Space

The algorithm was written in C++ to run on the on a Windows 95, PC operating system. The C++ programming language provides a fast and flexible object oriented paradigm ideal for governing the creation, manipulation and interaction of geometric objects such as vectors, rays, beams and planes. All theoretical objects in the model were represented in 3D world space (Hill[8]), i.e. in terms of positions and directions within a 3D coordinate system (x,y,z). Fundamental object types within the world space include

- Vectors – from which all other geometric objects were derived.

  $$v = (x, y, z) \qquad (1)$$

  where v is a vector and x,y,z are displacements in 3D world space.

- Polygons - represented by a series of vectors

  $$P = (v_1, v_2, v_3, \ldots) \qquad (2)$$

  where P is a polygon and V_1, V_2, V_3 are vectors.

- Planes –are polygons that are also represented by the equation of a plane

  $$n \cdot v_1 = D \qquad (3)$$

  where n is the unit normal to the plane and D is the plane coefficient.
  Planes also have associated sound absorption and diffusion coefficients.

- Rays - represented by source, direction and time components

$$r = s + ct \qquad (4)$$

where s is the ray source vector, c is unit direction vector and t is time travelled.

- Beams - consist of a collection of rays r_n that describe its shape

$$bm = (r_1, r_2, r_3, \ldots) \qquad (5)$$

Associated with every beam is it's source vector s_{bm} and an energy value E_b.

2.3 The Omni Directional Source

An icosahedron (Fig. 2) is used to create the initial twenty triangular beams of equal dimensions to describe the first order omindirectional sound field. An Icosahedron with 20 sides is defined by the twelve co-ordinates

(0,+/-F,+/-1), (+/-1,0,+/-F), (+/-F,+/-1,0) (6)

where F is the golden ratio ((sqrt(5)+1)/2=1.61803.

2.4 The Main Loop

Every beam is in turn passed to the main loop (Fig.3) that pushes the beam onto a stack, i.e. a temporary collection area where beams await processing. Each beam is in turn popped off stack and a point in beam test is used to determine if the detector is illuminated. Having removed irrelevant planes, the algorithm then tests for the nearest intersection of a beam's ray with a wall. This intersection will be the starting point for calculating first section of illumination and all other plane sections illuminated by the beam (see later). Each section of illumination is used to make a new reflected child beam. Reflected beams below a maximum order of reflection are pushed onto the beam stack to be popped off by the main loop later. The main loop continues to pop off and process beams until none are left.

2.5 Finding Sections of Illumination

Central to the adaptive beam tracing algorithm is it's ability to determine the exact sections of planes illuminated by a beam. These sections of illumination are subsequently used to determine the cross sections of reflected beams. Hence unlike triangular and conical beam tracing methods there are no gaps or overlaps in the predicted sound field.

As shown in Fig.4. the algorithm has to deal will all manner of illumination scenarios including single planes, multiple planes, corners, occluding planes and even planes that could cause holes in the reflecting beams. The algorithm uses the fact that the sides or edges of the beam and edges of every plane illuminated will determine the boundaries of illuminated sections (Fig.5). The progress of a 'Descriptor Ray' as bounded by 'Edge Planes' will be used to map out these sections of illuminations.

An Edge Plane is the extrapolation of a beam or plane edge to very large distance relative to the beam source. An Edge Plane can be represented by

$$P_e = (s_{bm}, v_1, v_2) \qquad (7)$$

where v_1 and v_2 the vertices of the edge extrapolated to a very large distance relative to the beam source s_{bm}. The Edge Plane can also be represented by its normal n_e and plane coefficient D where

$$D = n_e . s_{bm} \qquad (8)$$

A Descriptor Ray is the intersection of an Edge Plane with the plane being illuminated. Given it starts at an intersection s_d a Descriptor Ray can be represented by

$$r_d = s_d + c_d t \qquad (9)$$

Where c_d is as the cross product of an Edge Plane normal n_e with the illuminated plane normal n_p

$$c_d = n_e \times n_p \text{ or } c_d = n_p \times n_e \qquad (10)$$

The algorithm describes sections of illumination by

- finding the nearest plane intersecting with a beam's constituent ray
- creating a Descriptor Ray starting from this intersection with a direction given by intersection of the beam's Edge Plane with the illuminated plane surface
- finding the nearest valid Edge Plane the Descriptor Ray intersects
- using this intersection and nearest Edge Plane to create a new Descriptor Ray.

Hence, Descriptor Rays are used to find closed sections of illumination.

As the current section of illumination is mapped out extra Descriptor Rays are also created along any adjacent planes and occluding planes (Fig. 6.). These extra Descriptor Rays are set aside for the mapping of other sections illumination on other planes hence all sections on all illuminated planes are eventually found. Since the algorithm tests for any Descriptor Rays covering old ground, no section is described twice.

For descriptor rays to map out sections of illumination they must follow the correct sense, i.e. clockwise or anticlockwise relative to the beam source. The sense of the Descriptor Ray is dependant on the sense of the beam and any planes it may encounter. Sense can be determined using cross product and triple scalar product. Given three concurrent vertices of a plane v_1, v_2, v_3 and the beam source s_{bm}, then it can be shown that the triple scalar product T indicates the plane sense.

$$T = (v_2 - s_{bm})((v_2 - v_1) \times (v_3 - v_2)) \qquad (11)$$

$T > 0$ is a positive clockwise turn and $T < 0$ is a negative anticlockwise turn

For the beam tracing algorithm to cope with sense correctly, all planes and beam cross-sections must be convex. Concave polygons are detected by testing for the preservation of sense, and subsequently divided into convex subsections. To ensure the correct sense of the description process a large set of sense rules governing the direction of the Descriptor Ray had to be determined and implemented. These sense rules form the crux of the function to determine the best direction the Descriptor Ray.

When a Descriptor Ray encounters a corner a number of edge planes may be intersected simultaneously hence there may be number of possible directions the new Descriptor Ray may take. The intersected edge creating the sharpest turn will correspond to the correct mapping since it will represent the current plane boundary or an occluding plane.

Any plane lying completely within a beam was tested for, so as to eliminate the possibility of holes within the reflected beam cross-section. When such a plane is encountered the beam is subdivided with respect to a point on the plane and the resulting child beams pushed onto the beam stack.

2.6 Detector Illuminated

Determining if the detector is illuminated by a beam was done by creating a ray that originates from the current beam source passing through the detector. If this ray intersects with a visible beam cross section then the point is within the beam. When the detector is illuminated by a beam the current beam energy and ray time is stored. Hence, as child beams are created and reflected an echogram of the room is compiled.

2.7 Reflecting Beams

Creating reflected child beams requires finding the image of the parent beam source in the reflecting plane. Given that the distance or time t of the beam source s from a plane is

$$t = p - s \bullet n \qquad (12)$$

Then the image of the beam source s_i relative to the plane is

$$s_i = p + 2tn \qquad (13)$$

For each section of illumination new beam rays are created that intersect with it's respective vertices and originate from the new beam source (Fig. 7.).

Upon reflection specular beam energy is lost to wall absorption and the diffuse system. Hence given the parent beam energy E_b, the wall absorption coefficient α and diffusion coefficient δ the reflected beam energy E_r is

$$E_r = E_b(1-\alpha)(1-\delta) \qquad (14)$$

Note that the beam energy in the specular model is essentially the original source energy minus energy lost to wall absorption and diffusion after reflections. The beam serves as a detector finder its specular energy value being independent of the beam's cross-sectional area. On finding the detector the energy incident on the detector takes account of $1/r^2$ and air attenuation, where r is the distance the beam has travelled.

The diffuse model requires the proportion of diffuse sound energy that the beam has imparted to the wall with respect to time and so is dependant on the beam's cross-sectional area. This energy is proportional to $\frac{\Delta\Omega}{\Omega}$, where $\Delta\Omega$ is the solid angle subtended by a area of illumination and Ω is the solid angle subtended by a sphere. The solid angle subtended by the beam is calculated by extrapolating all constituent beam rays to an equal arbitrary distance L, hence the resulting extrapolated polygon of area A is used to determine the proportion of energy incident E_d, as shown by Equation 15.

$$E_d \propto \frac{\Delta\Omega}{\Omega} E_b\, \delta(1-\alpha) \propto \frac{E_b A \delta(1-\alpha)}{4\pi L^2} \qquad (15)$$

2.8 The Diffuse System

During the specular beam tracing process, time and plane dependant energy information passes to the diffuse system (Fig. 8.).

Every wall is assigned a plane impulse response that serves as a record of diffuse energy imparted by beams with respect to time. The plane impulse response consists of energy bins at discrete time intervals Δt. When a beam is incident on a wall the imparted beam energy E_d is added to the time bin corresponding to the average time the beam has travelled.

Upon completion of the specular beam tracing a separate diffuse sound profile is calculated using a radiant exchange process. For every time interval of every plane impulse response, the corresponding diffuse energy is re-radiated to all other planes (Fig. 9.). Each receiving plane hence has a proportion of this energy added to its plane impulse response at a time interval corresponding to an average distance between the radiating and receiving planes. These energy portions received will in turn be re-radiated to other planes later on during the exchange process and so on. The exchange process cycles through successive time intervals redistributing energy until an arbitrary time that is much greater that the maximum selected order of beam reflection. How much diffuse energy each plane receives is dependant on a form factor between the radiating and receiving planes. The plane form factor F_{ij} between two planes is the fraction of energy diffusely emitted from surface *i* that reaches surface *j* as given by Equation 16.

$$F_{ij} = \frac{1}{A_j} \int_{A_i}\int_{A_j} \frac{\cos\theta_i \cos\theta_j}{\pi r^2}\, dA_i A_j \qquad (16)$$

where A_i is the surface area of the emitting surface, r is the length of the line joining the two elemental areas and θi and θj are the angles formed between this line and the respective plane normals. The form factor be calculated as the average solid angle subtended by the receiving plane relative to grid of points on the radiating plane.

When the radiant exchange process is completed diffuse energy at the detector can be calculated. For each time interval of each plane impulse response diffuse energy is re-radiated to the detector. Hence a diffuse impulse response at the detector is built up allowing for the forms factors and distances between the detector and radiating planes.

The adaptive beam tracing algorithm like all other methods can only calculate specular reflections to a finite order, hence remaining energy is assumed to pass to a totally diffuse system to be later used in radiant exchange. This can be implemented by assuming plane diffusion coefficients have the value 1 for high orders of reflection. However, an abrupt crossover can leave artefacts in the predicted sound decay curve. Thus, a more gradual crossover to totally diffuse over a range of high order reflections was implemented.

2.9 Recombining Specular and Diffuse Components

Given specular and diffuse impulse responses the two must be combined to produce an accurate profile of the room's acoustics.

Clarity and Deulikiet can be calculated simply by integrating specular and diffuse energies with respect to time.

$$C_{80} = 10\log_{10}\frac{\int_{0}^{80ms} E(t)dt}{\int_{80ms}^{\infty} E(t)dt} \tag{17}$$

In order to calculate Reverberation Time and Early Decay Time a profile of sound energy decay is needed. This is done combining specular and diffuse impulse responses. Then using a backwards integration method Schroeder[9] a decay profile is built up (Fig.10). A linear regression on the resultant curve can be used to determine RT and EDT.

3 Comparisons with Other Methods and Real Measurements

3.1 Comparison with the Image Method and Ray Tracing

Comparisons of the adaptive beam tracing algorithm for accuracy and speed were made with an implementation of ray tracing and of the image method. All methods were tested with the same hall data to produce a specular echogram of sound energy incident on the detector with respect to time. The ray tracing algorithm was implemented to use a spherical detector hence a record of rays intersecting was built up. Rays with same plane to plane path would sometimes be recorded while other valid ray paths missed. These systematic errors for ray tracing were demonstrated by Lehnert[2] who subsequently suggested a criterion for ray density based on detector size and the mean free path of the hall. The image method used was based on an efficient algorithm (Lee and Lee[4]) which takes account of obstructions and invalid images.

Given hall data for a simple concert hall with a stage and balcony (Fig. 11.) impulse responses were predicted for the adaptive beam tracing algorithm, the image method and ray tracing (Fig. 12.). The beam tracing algorithm correlates well with the image method implemented without exhibiting the degree of duplicated and missing images predicted with ray tracing. This implementation of adaptive beam tracing may very occasionally miss a reflection due to calculation ambiguities during the mapping out of areas of illumination also the image method may generate spurious images within the balcony volume. However both cases are very rare and have a negligible bearing on the final results.

Comparisons of calculation time were made for the three methods using a relatively slow 486 personal computer. Fig. 13 shows that Ray Tracing can be fast with an arbitrary number of rays used across a range of orders of reflection, however systematic errors increase. By applying an error criterion to specify the number of rays used for a given detector size (Lehnert[2]), ray tracing was demonstrated to be much slower than beam tracing. The image method is the fastest for low orders of reflection, however calculation times increase exponentially with orders of reflection or number of planes used. Hence, beam tracing is the fastest algorithm for all but the lowest orders of reflection or simplest of halls.

3.2 Comparison with Measured Data

The adaptive beam tracing algorithm was applied to a number of real halls for comparisons with measured results. For example measurements of Reverberation Time, Early Decay Time, and Clarity Index were made across a range of frequencies for a lecture hall that is also used for music performances (Fig. 14.). The adaptive beam tracing algorithm was implemented on a representation of this hall based on architectural data and known surface absorption coefficients. The use of this hall data demonstrates the algorithm's ability to handle relatively complex models that include reflectors and obscuring planes. The walls, ceiling and reflectors were assumed to have a diffusion coefficient of 0.1. Soft seating was assumed to have a diffusion coefficient of 0.7. These were values estimated in an earlier study (Howarth[10]). For each frequency the algorithm calculated RT, EDT and C80. The results for R.T. (Fig 15) show a good correlation with measured although usually less than predicted demonstrating a possible loss of predicted energy for higher orders of reflection. However this may impart be due to an over estimation of absorption coefficient and the algorithm ignoring hall resonance and outside noise like traffic. The results for E.D.T. (Fig. 16) and C80 (Fig 17.) show some variance with frequency. These can be improved by calculating to higher orders of reflection although at the expense of fast computation.

4 Conclusions

The adaptive beam tracing algorithm shows improvements in speed over the image method and ray tracing. The algorithm seeks to eliminate systematic errors resulting from overlaps and omissions in predicted sound propagation whilst facilitating an integrated calculation of specular and diffuse systems so removing the need for statistical and empirical adjustments. The algorithm copes well with many hall scenarios by inherently dealing with occluding planes. However, relative to ray tracing and the image method the adaptive beam tracing algorithm is difficult to implement relying on sophisticated techniques to map out sections of illumination. Certain complicated plane alignments can confuse the algorithm creating effects similar to optical illusions. Hence the algorithm must be able to deal with these by using a degree of artificial intelligence. There is plenty of scope to improve the algorithm's reliability and efficiency.

In conclusion the adaptive beam tracing algorithm provides a logical and complete way to model sound propagation. Though difficult to implement the algorithm has many advantages over existing methods.

5 References

1 A. Kulowski, "Algorithmic Representation of the Ray Tracing Technique," Applied Acoustics 18, 449-469, (1984)

2 H. Lehnert, "Systematic Errors of the Ray-Tracing Algorithm," Applied Acoustics 38, 207-221, (1993)

3 J. Borish, "Extension of the Image Model to Arbitrary Polyhedra," J. Acoust. Soc. Am. 75 (6), 1827-1836, (1984)

4 H. Lee & B. Lee, "An Efficient Algorithm for Image Method Technology," Applied Acoustics 24, 87-115, (1988)

5 M. Volander, "Simulation of Transient and Steady State Sound Propagation in Rooms using a New Combined Ray Tracing / Image Source Algorithm," J. Acoust. Soc. Am., 86 (1), (1989)

6 D. Van Maercke & J. Martin, "The Prediction of Echograms and Impulse Responses within the Epiduare Software", Applied Acoustics 38, 93-114, (1993)

7 T. Lewers, "A Combined Beam Tracing and Radiant Exchange Computer Model of Room Acoustics," Applied Acoustics," 38, 161–178, (1993)

8 F.S. Hill, *Computer Graphics*, (Macmillan, New York, 1990), pp. 305-424

9 M. R. Schroeder, "New Method for Measuring Reverberation Time," J. Acoust. Soc. Am. **37**, 409-412, (1965)

10 M. J. Howarth, "The Application of Advanced Computer Models to the Prediction of Sound in Enclosed Spaces", PhD Thesis, The University of Salford, UK, 1998

Fig.1. A beam traced adaptively

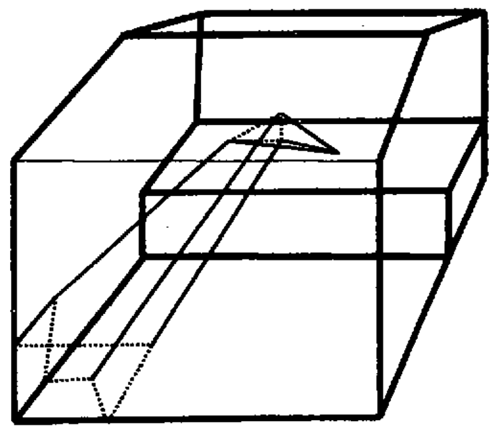

Fig.2. An icosahedron used for creating an omnidirectional source

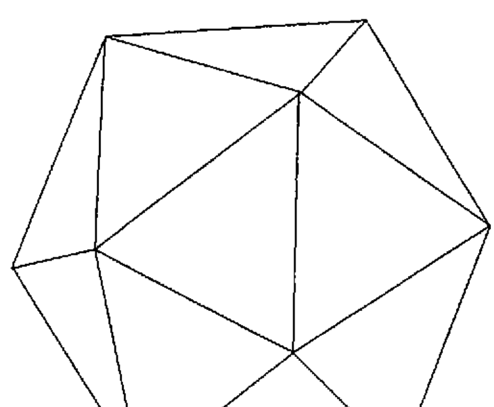

Fig.3. Schematic diagram for main loop of beam tracing algorithm

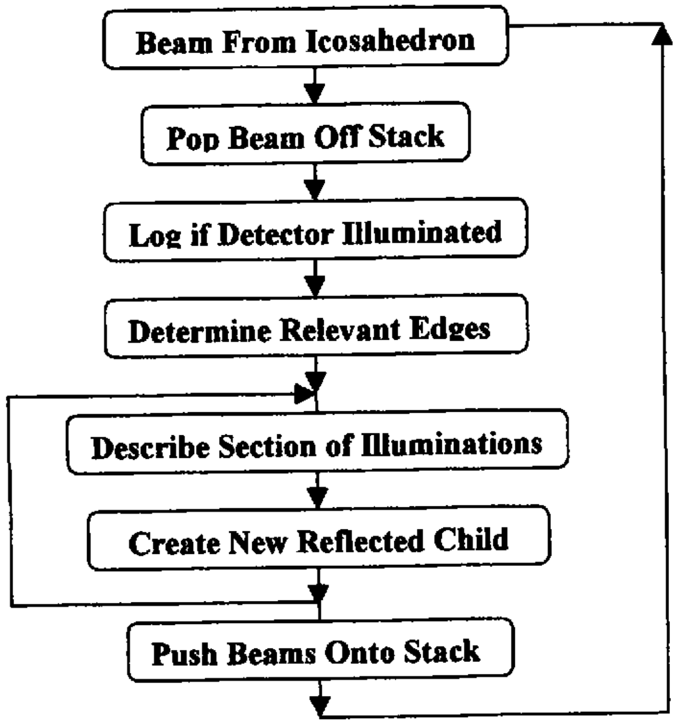

Fig.4. Different ways in which a beam can illuminate planes

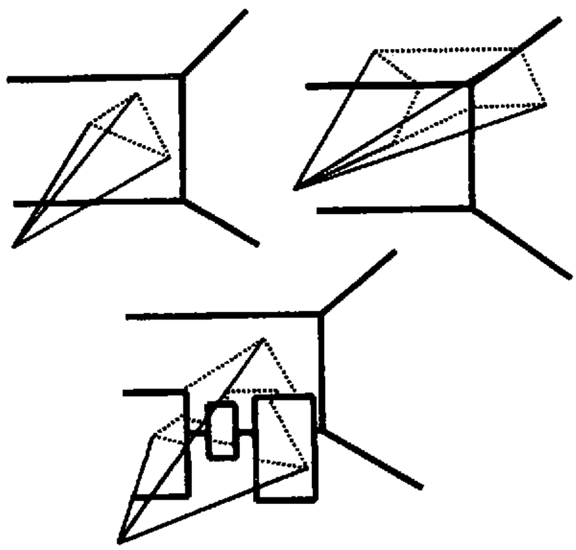

Fig.5. How the edges of planes determine sections of illumination

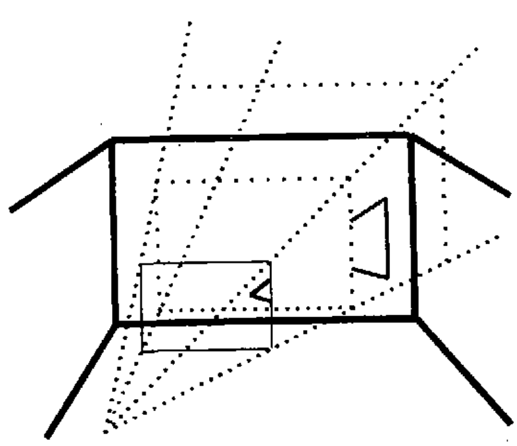

Fig.6. Descriptor rays mapping out section of illumination. During this process adjacent sections illuminated by the beam are found with new starting descriptor rays being set aside for subsequent mapping.

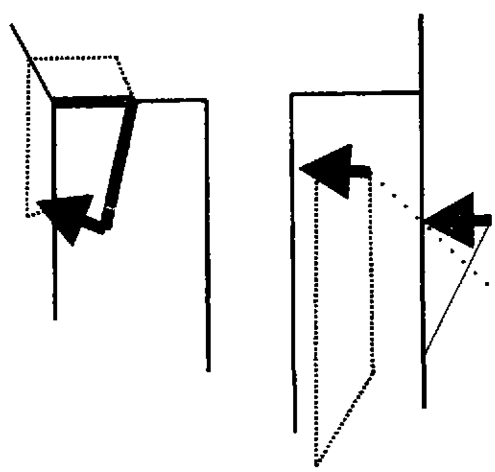

Fig.7. A reflected child beam constructed from the beam source image of the parent beam and the vertices of the area of illumination

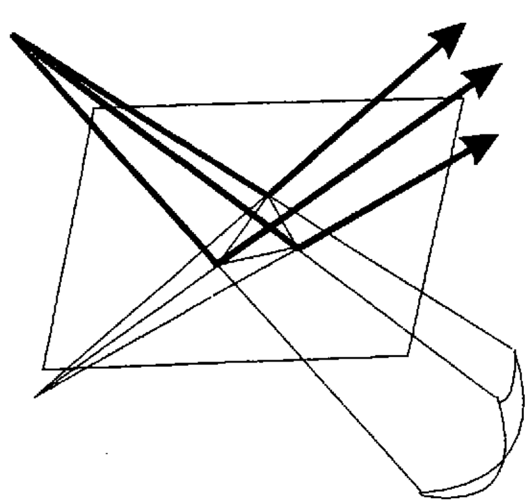

Fig.8. Schematic diagram representing the relationship between specular and diffuse models

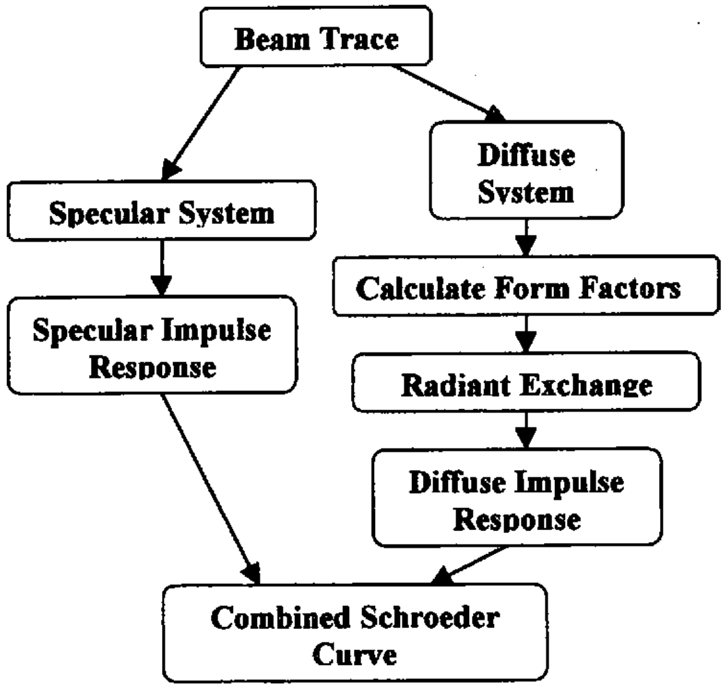

Fig.9. Diffuse energy from plane re-radiated to other planes

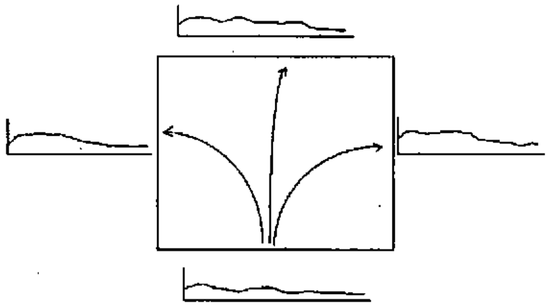

Fig.10. Sound Pressure Level decay profile as determined by backwards integration

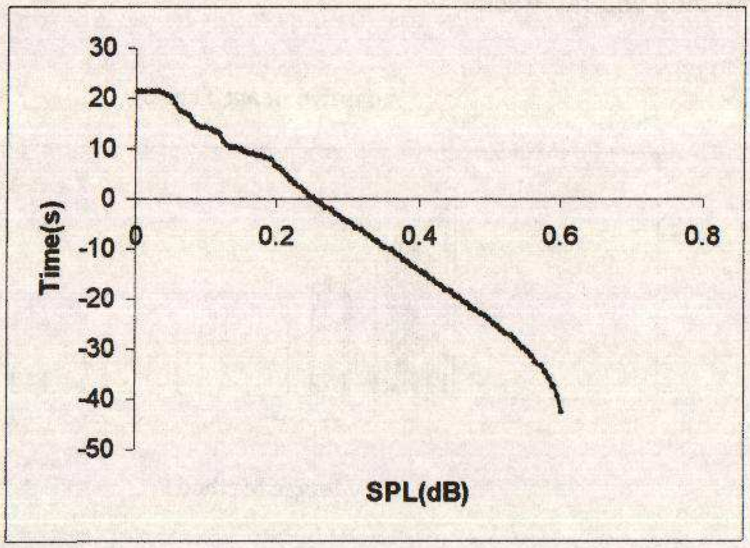

Figure 11: Concert hall with stage area and balcony ~ 32m x 24m x 13m

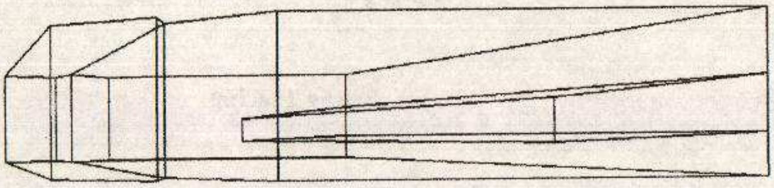

Figure 12: Predicted impulse responses for hall using adaptive beam tracing, the image method and ray tracing

Adaptive Beam Tracing

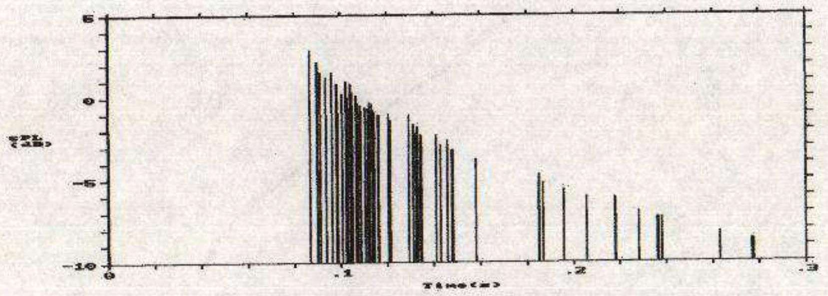

Image Method

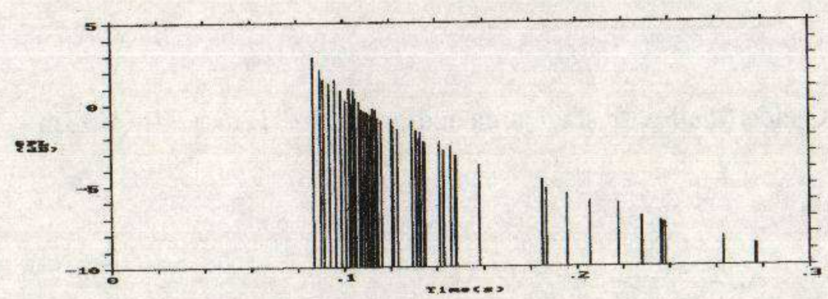

Ray Tracing

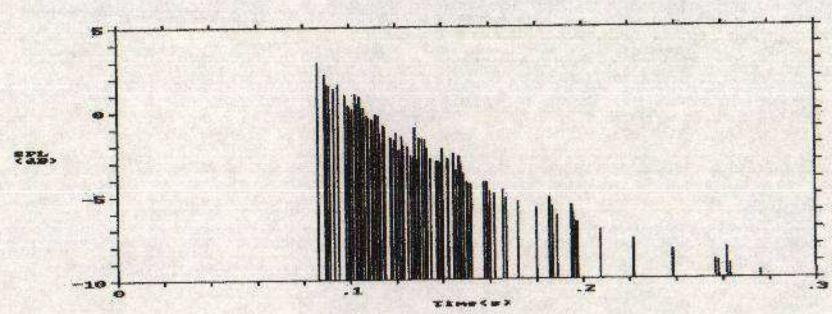

Figure 13: Time profiles for adaptive beam tracing, the image method and ray tracing

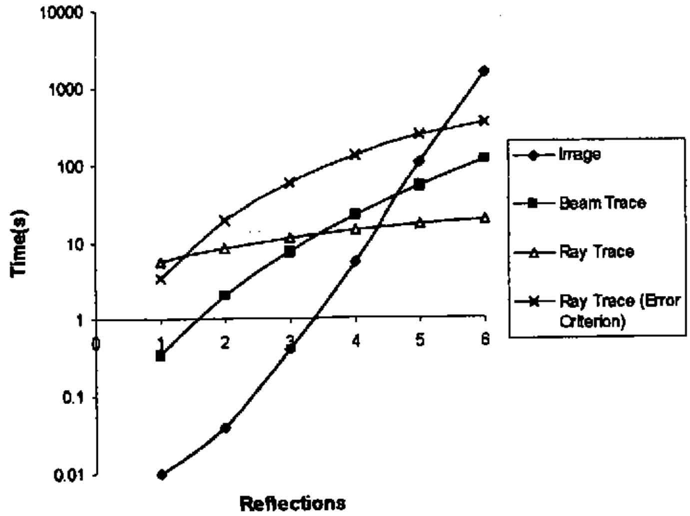

Figure 14: Sheffield Hallam Concert Hall ~ 23m x 19m x 8m

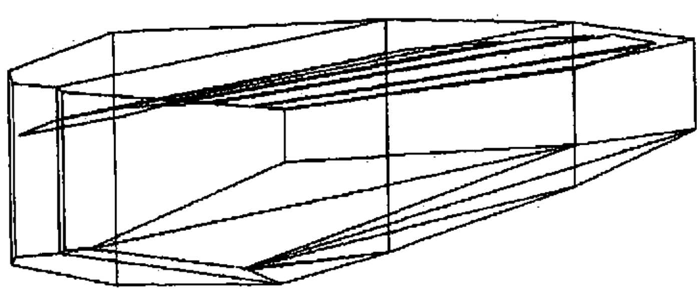

Figure 15: Comparisons of Measured and Predicted R.T.s for Sheffield Hallam Concert Hall

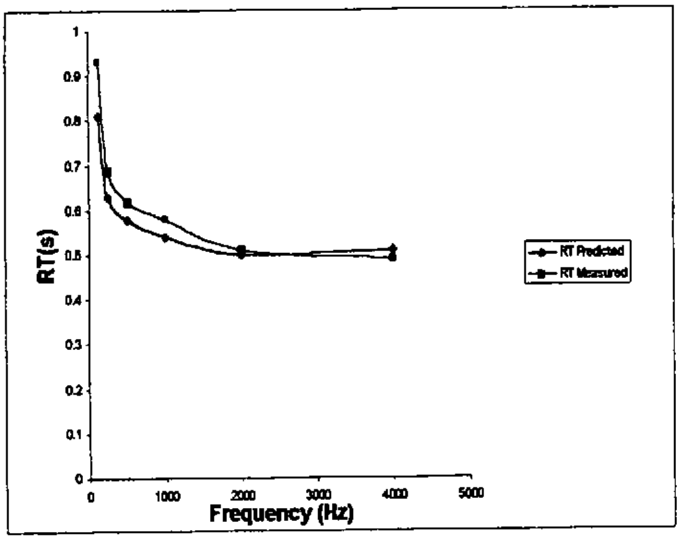

Figure 16: Comparisons of Measured and Predicted E.D.T.s for Sheffield Hallam Concert Hall

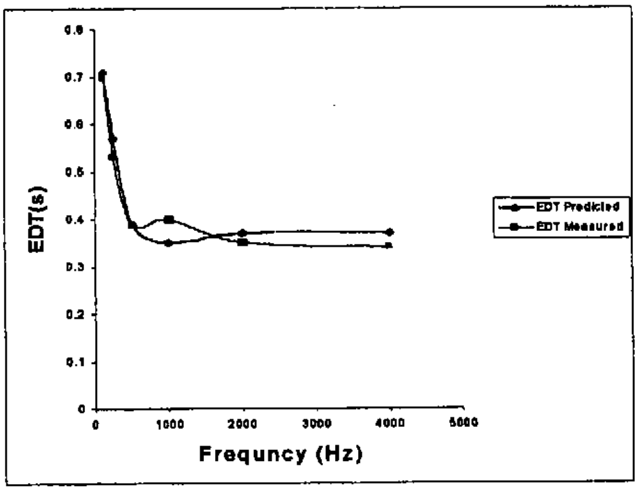

Figure 17: Comparisons of Measured and Predicted C80s for Sheffield Hallam Concert Hall